First publ. in: Physical Review B ; 86 (2012), 3. - 035118
DOI : 10.1103/PhysRevB.86.035118

Spectral dependence of the magnetic modulation of surface plasmon polaritons in noble/ferromagnetic/noble metal films

Diana Martín-Becerra,[1,*] Vasily V. Temnov,[2,†] Tim Thomay,[3,‡] Alfred Leitenstorfer,[3] Rudolf Bratschitsch,[3,§] Gaspar Armelles,[1] Antonio García-Martín,[1] and María Ujué González[1,∥]

[1]*IMM-Instituto de Microelectrónica de Madrid (CNM-CSIC), Isaac Newton 8, PTM, E-28760 Tres Cantos, Madrid, Spain*
[2]*Department of Chemistry, Massachusetts Institute of Technology, Cambridge, Massachusetts 02139, USA*
[3]*Department of Physics and Center for Applied Photonics, University of Konstanz, D-78457 Konstanz, Germany*

(Received 21 March 2012; revised manuscript received 1 June 2012; published 12 July 2012)

The magnetic field is an interesting candidate for the development of active plasmonic devices as it is able to modify the surface plasmon polariton (SPP) wave vector. Both real and imaginary parts of the SPP wave vector are affected. Here, we have experimentally determined the contribution of both modulations in the spectral range $\lambda_0 = 500$–1000 nm for magnetoplasmonic systems consisting of noble/ferromagnetic/noble multilayered metal films. We have seen that the real part usually exceeds the imaginary one, but in the longer wavelength range the contribution of the imaginary part cannot be neglected. We have analyzed the spectral dependency of the modulation, and we conclude that it is dominated by the evolution of the SPP properties with wavelength and not the magneto-optical parameter. A figure of merit including modulation and propagation distance is also studied for the three ferromagnetic metals, Fe, Co, and Ni.

DOI: 10.1103/PhysRevB.86.035118 PACS number(s): 75.70.Cn, 71.36.+c, 73.21.Ac, 73.20.Mf

I. INTRODUCTION

The increasing demand of our society for faster communication networks and information-processing systems, being at the same time more efficient or greener in terms of energy consumption, constitutes a key driving force towards the progress of integrated photonic devices. The design and fabrication of new nanoscale optical systems becomes therefore crucial in order to deliver all the different functions required in these devices. Surface plasmon polaritons (SPPs) are propagating electromagnetic waves bound to a metal-dielectric interface, therefore vertically confined. Besides, they can be laterally confined beyond the diffraction limit by nanostructuring the interface. Recent advances in SPP-based (plasmonic) systems, with a wide range of passive coupling and guiding elements demonstrated, show that they are one of the relevant candidates to achieve these nanophotonic circuits,[1–4] provided that the intrinsic loss of the system can be overcome by using appropriate gain strategies.[5] Furthermore, important progress has been made in the last years to achieve active plasmonic configurations,[6–18] i.e., plasmonic systems that could be externally manipulated, which is a critical step to really endow plasmonic systems with full capacity of development of nanophotonic chips as it will allow the realization of fundamental components such as modulators, switches or active multiplexors, couplers, and add-drop filters. Several external agents have been proposed so far to provide the controlled response of these active plasmonic systems: temperature,[6,7,14] voltage,[10,11,17,18] optical signals,[8,9,12,13] or magnetic field.[15,16] In all cases, the mechanism underlying the modification of the system's response is either the control of absorption[6,8,9,11,17] or the modification of the material refractive index and thus of the SPP wave vector[7,10,14–16,18] (a combination of both in some specific cases[12,13]).

The use of magnetic field and associated magneto-optical (MO) effects as the driving agent can be of particular interest because of its flexibility. It has been known since the early seventies that a magnetic field $\mathbf{B} = B_0\hat{\mathbf{x}}$ parallel to the interface induces a modification on the wave vector of a SPP traveling in the perpendicular direction, $\mathbf{k}_{sp} = k_{sp}\hat{\mathbf{y}}$ [see sketch in Fig. 1(a) for relative directions]:[19–21]

$$k_{sp}(\pm B_0) = k_{sp}^0 \pm \Delta k_{sp}(B_0), \tag{1}$$

where k_{sp}^0 is the SPP wave vector without applied magnetic field and Δk_{sp} is the modulation induced by the magnetic field, which is related to the off-diagonal element of the dielectric tensor ϵ_{yz}, also called MO constant. This modification occurs in both the real and imaginary part of k_{sp}: k_{sp}^r (Δk_{sp}^r) and k_{sp}^i (Δk_{sp}^i), respectively. The amount of modulation of each part is different, and is a function of the optical and MO properties of our particular system. The real and imaginary parts of k_{sp} represent different physical properties: k_{sp}^r accounts for the SPP phase velocity while k_{sp}^i is related to its propagation distance. Therefore, the magnetic field offers the opportunity of designing active plasmonic systems based on the control of absorption if Δk_{sp}^i dominates, or on effective refractive index modification if Δk_{sp}^r does. Moreover, as can be seen in Eq. (1), the SPP modification under an applied magnetic field is nonreciprocal [$k_{sp}(B_0) \neq -k_{sp}(B_0)$], thus making this kind of system very interesting for the design of integrated optical isolators,[22–26] another fundamental piece for the development of nanophotonic circuits. Another advantage of the magnetic field driven systems is related to its potential switching speed, as it has been recently demonstrated that materials magnetization switching is an ultrafast phenomenon that can achieve the terahertz regime.[27]

The implementation of magnetic field induced modulation on plasmonic systems in the optical regime requires the use of materials combining good properties in terms of plasmon propagation and MO constant of sizable value. Unfortunately, noble metals have a quite small MO constant, so a magnetic material has to be introduced in the system to increase this response. Ferromagnetic metals seem an appropriate choice as they also support plasmons due to their metallic nature; however, their high optical absorption induces an excessive

 ©2012 American Physical Society

Konstanzer Online-Publikations-System (KOPS)
URN: http://nbn-resolving.de/urn:nbn:de:bsz:352-217099

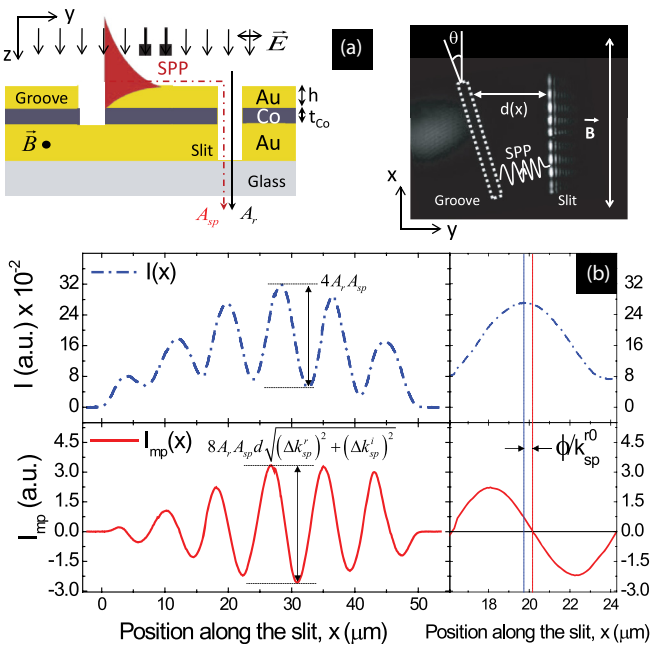

FIG. 1. (Color online) (a) Left side: Sketch of the magnetoplasmonic interferometer with definition of the system geometry and structural parameters. Right side: Image from the slit back side, showing the transmitted intensity interference pattern resulting from the interference between the light directly transmitted through the slit and the surface plasmon polariton excited at the groove and decoupled at the slit after having traveled the groove-slit distance. (b) Optical (top panel) and magnetoplasmonic (bottom panel) interferograms for an interferometer with the following particular geometry: slit-groove angle $\theta = 5^\circ$, minimum slit-groove distance $d(0) = 20\ \mu$m, AuCoAu trilayer of $h = 25$ nm. The measurements correspond to $\lambda_0 = 633$ nm. The right side inset shows a zoomed portion of both interferometers to depict in more detail the phase shift, ϕ.

damping of the SPP propagation which prevents their use as the only metallic component of the system. This has led to the combination of noble and ferromagnetic metals as suitable magnetoplasmonic systems.[15,16,28–31] The possibility of realizing magnetic field driven SPP modulators has been recently demonstrated using this kind of system.[15] Moreover, the modulation can be increased with the addition of a thin dielectric layer on top of the metallic multilayer,[16] or by optimizing the quality of the interfaces.[31] A deeper understanding of the behavior of these systems would allow for a further development of active plasmonic devices acting through a magnetic field.

In this paper, we have experimentally determined the spectral evolution of the modulation of both the real and imaginary parts of the SPP wave vector in the visible and near-infrared (from 500 nm to 1 μm) for Au/Co/Au multilayered systems. As will be shown, the relative weight of each part depends on the wavelength range, so this aspect has to be taken into account to optimize the obtained response in these systems. We also analyze the dependence of both modulations on the different optical and magneto-optical parameters of the system, expanding the study to other ferromagnetic metals. We have found that the spectral behavior of Δk_{sp} is dominated by the evolution of the SPP properties, namely the vertical spreading of the evanescent wave. Finally we discuss the optimum spectral range for application purposes in terms of a figure of merit combining both modulation and SPP propagation distance.

II. EXPERIMENTAL DETERMINATION OF Δk^r_{sp} AND Δk^i_{sp}

The values of the real and imaginary part of the SPP wave vector modulation induced by the magnetic field have been obtained by means of plasmonic microinterferometry with tilted groove-slit arrangement,[13] using the same configuration as that employed for the implementation of magnetoplasmonic modulators.[15,16] A sketch of this configuration is shown in Fig. 1(a): A slit and a tilted groove have been engraved by means of a focused ion beam (FIB) on a Au/Co/Au trilayer (total thickness 200 nm). The thickness of the Co layer, t_{Co}, is 6 nm, and it is placed at different depths from the trilayer surface ($h = 15$, 25, and 35 nm). The slit, of width 100 nm, goes through all the metal thickness, while the groove, 200 nm wide, has a depth of around 100 nm. These dimensions, although not optimized for maximum coupling or resonant transmission of SPPs at each wavelength,[32] have allowed us to satisfactorily excite and detect the surface plasmon polaritons in all the aimed spectral range, from 500 nm to 1 μm. When illuminating the interferometer with a p-polarized laser beam, the light collected at the back side of the slit results from the interference between light directly transmitted through the slit and light originating from a surface plasmon polariton that has been excited at the groove, has traveled towards the slit, and is decoupled in the slit. This transmitted light intensity can be expressed as

$$I = A_r^2 + A_{sp}^2(x) + 2A_rA_{sp}(x)\cos\left[k^r_{sp}d(x) + \varphi_0\right], \quad (2)$$

where A_r corresponds to the field amplitude of the light passing directly across the slit and A_{sp} to that associated with the SPP. Due to the tilted groove-slit configuration, the distance d between them depends on the position along the slit, $d(x)$, and the optical path difference entering in the cosine argument changes, which results in a pronounced interference pattern along the slit axes, as can be seen in Fig. 1(a). The SPP related field amplitude A_{sp} also depends on $d(x)$ because of the damping during SPP propagation, $A_{sp}(x) = A^g_{sp}e^{-k^i_{sp}d(x)}$, where A^g_{sp} is the amplitude of the excited SPP at the groove position, which in principle is, as A_r, constant along the groove. The phase φ_0 is a constant phase arising during SPP coupling at the groove and uncoupling at the slit. We collect the intensity at the back side of the slit by scanning a photodiode along a projected image obtained with a 20× long-distance objective. This signal constitutes the optical interferogram, and an example corresponding to an interferometer with slit-groove angle $\theta = 5^\circ$ and minimum slit-groove distance $d(0) = 20\ \mu$m in a AuCoAu trilayer of $h = 25$ nm, measured at $\lambda_0 = 633$ nm, is plotted in the top panel of Fig. 1(b).

If an external periodic (1.4 kHz in our experimental configuration) magnetic field high enough to saturate the sample ($B \approx 20$ mT) is applied parallel to the sample interface and along the slit axis, a modification in the SPP wave vector is induced following Eq. (1), which results in a modification of the optical path difference and therefore a shift in the interference pattern. This leads to a variation of the transmitted

intensity at each point of the slit synchronous with the applied magnetic field, $\Delta I = I(+M) - I(-M) \equiv I_{mp}$. In a first-order approximation, this intensity variation corresponds to the derivative of the transmitted intensity I with respect to the magnetic field, and it can be expressed as

$$I_{mp} = -4A_r A_{sp} d\sqrt{\left(\Delta k_{sp}^r\right)^2 + \left(\Delta k_{sp}^i\right)^2}\sin\left(k_{sp}^{0r} d + \varphi_0 + \phi\right), \tag{3}$$

where k_{sp}^{0r} and k_{sp}^{0i} are the real and imaginary parts of k_{sp} when there is no magnetic field applied. This intensity variation is collected with the scanning photodiode by using lock-in detection and constitutes the magnetoplasmonic interferogram [see bottom panel of Fig. 1(b)]. It can be seen that I_{mp} is proportional to the modulus of Δk_{sp} and to the distance covered by the plasmon d. Moreover, I_{mp} is phase shifted with respect to I: The modulation of k_{sp}^r induces a $\pi/2$-phase shift, and the presence of Δk_{sp}^i adds an additional ϕ phase, defined as $\tan\phi = \Delta k_{sp}^i/\Delta k_{sp}^r$ [a full derivative of Eq. (3), with the explicit contribution of Δk_{sp}^r and Δk_{sp}^i, can be found in the Appendix]. By determining the phase shift between both interferograms and the ratio of the amplitude of the magnetoplasmonic signal to the amplitude contrast of the optical one [shown in Fig. 1(b)], both the real and imaginary parts of the SPP wave vector modulation can be determined.

III. SPECTRAL BEHAVIOR OF Δk_{sp}^r AND Δk_{sp}^i

In order to analyze their spectral dependence, we have measured Δk_{sp}^r and Δk_{sp}^i by illuminating the magnetoplasmonic interferometers with several lasers of different wavelengths ($\lambda_0 = 532$, 633, 680, 785, 860, and 890 nm). The obtained results are plotted in Fig. 2 (filled symbols) for three trilayers where the Co layer is placed at different positions, $h = 15$, 25, and 35 nm. The upper graph corresponds to the real part of the modulation, and the lower graph to the imaginary part. Together with the experimental results, Fig. 2 also includes, as dashed lines, the values of Δk_{sp}^r and Δk_{sp}^i obtained from numerical simulations performed in the following way:[33] Our multilayered air/Au/Co/Au/glass system is modeled by means of a transfer matrix formalism where the magneto-optical activity is accounted for by describing the Co layer with the corresponding dielectric tensor. Then, a numerical solver for guided modes is applied to find the SPP supported by the metal-air interface in the presence and absence of an applied magnetic field **B**. The optical and MO constants of the different materials involved have been obtained by ellipsometric and polar Kerr characterization,[29] respectively, of the samples containing the interferometers. As can be seen, the agreement between the experiment and the simulations is very good.

As Fig. 2 shows, the general trend for both real and imaginary part wave vector modulations is that the modulation value decreases with wavelength, an unexpected behavior in principle as the absolute value of the MO constants of Co increase with wavelength [see Fig. 3(a)], and whose origin will be discussed in detail in the next section. The same behavior is obtained for all three different positions of the Co layer,

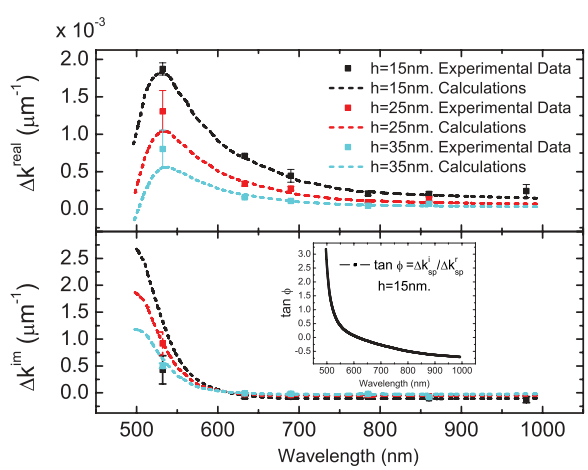

FIG. 2. (Color online) Wavelength dependence of Δk_{sp}^r (top graph) and Δk_{sp}^i (bottom graph) obtained for magnetoplasmonic trilayers with three different positions of the Co layer, $h = 15$, 25, and 35 nm. The filled symbols correspond to experimental values and the dashed lines to values obtained numerically. The inset shows the calculated ratio $\Delta k_{sp}^i/\Delta k_{sp}^r$, which corresponds to $\tan\phi$.

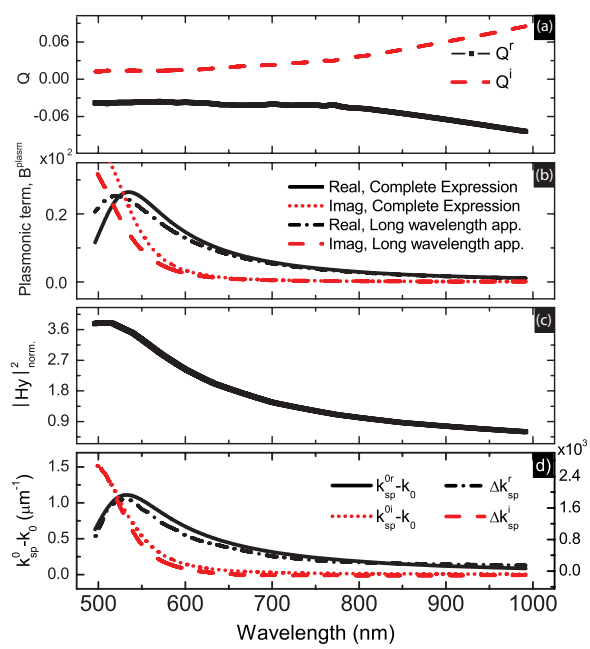

FIG. 3. (Color online) (a) Wavelength dependence of the magneto-optical parameter Q for our Co layers, as obtained from ellipsometric and polar Kerr characterization. (b) Evolution of the plasmonic term from the analytical expression of Δk_{sp} for the AuCoAu trilayers. Both the long-wavelength approximation (real part in black dash-dot line and imaginary part in dashed red line) and complete expressions (real part in black solid line and imaginary part in dotted red line) are plotted. (c) Spectral dependence of the intensity of the SPP magnetic field at the middle of the Co layer in a AuCoAu trilayer with $h = 15$ nm. The SPP magnetic field intensity is normalized in such a way that the intensity integrated along the z axis is 1 for each wavelength. (d) Evolution with wavelength of the separation of the SPP wave vector from the light line (left axis; real part in black solid line and imaginary part in red dotted line) compared with the evolution of Δk_{sp} (right axis; real part in black dash-dot line and imaginary part in dashed red line) for a AuCoAu trilayer (in particular, the case for $h = 15$ nm is plotted).

with the only difference of getting smaller absolute values of modulation as the Co layer lies deeper in the trilayer. This is due to the evanescent nature of the SPP: Its electromagnetic field decays exponentially inside the metal, and therefore the deeper the Co (ferromagnetic) layer the less electromagnetic field and as a consequence the less magnetic modulation would be achieved.[15]

Regarding the real part of Δk_{sp}, it presents a peak at low wavelengths ($\lambda_0 = 530$ nm).[34] This peak is not associated with a resonant behavior but with the presence of absorption in the metal, which makes the SPP dispersion relation bend around this wavelength close to the surface plasmon resonance frequency[35] (the discussion in the next section will clarify this point). As for the imaginary part, it is in general smaller than the real part in most of the spectral range. Only in the smallest wavelength part ($\lambda_0 < 520$ nm), again close to the surface plasmon resonance frequency, the imaginary part dominates. At this wavelength range, there is a discrepancy between theory and experiment, mainly due to the very short SPP propagation distance, which worsened significantly the signal-to-noise ratio during experiment. Taking into account the ratio between imaginary and real part modulations, shown in the inset included in Fig. 2, three spectral regions can be defined. For lower wavelengths ($\lambda_0 < 520$ nm), the dominant part of the modulation is the imaginary one, but this is a region where plasmon losses are too high to envisage any practical application of these systems. For the central range, between $\lambda_0 = 550$ nm and around 750 nm, the relevant component of the modulation is the real part, the imaginary one being a small perturbation that can be discarded ($\tan\phi \approx 0$), as was done in previous studies of the magnetoplasmonic modulators.[15,16] Finally, for the long-wavelength region the ratio increases, so that the imaginary part has to be taken into account in order to accurately describe the system. For example, in magnetoplasmonic modulators implemented in the form of interferometers and therefore based on the intensity variation given by Eq. (3), the contribution of Δk_{sp}^{i} is important to find the slit-groove distance of maximum response, as ϕ can no longer be neglected.

IV. DISCUSSION ON THE DIFFERENT FACTORS GOVERNING Δk_{sp}

To gain a deeper understanding on the obtained spectral behavior of the modulation of k_{sp}, an equation relating the implied parameters is necessary. An analytical expression for Δk_{sp} in a noble/ferromagnetic/noble metal trilayer can be obtained considering that the ferromagnetic layer (Co here) is very thin and that the MO activity is a small perturbation in the system ($|\epsilon_{yz}| \ll |\epsilon_{xx}|$):[15]

$$\Delta k_{sp} \approx 2t_{\mathrm{Co}} e^{-2hk_z^{\mathrm{Au}}} \times \frac{k_0^2 \epsilon_d^2 \epsilon_{\mathrm{Au}}^2}{(\epsilon_d^2 - \epsilon_{\mathrm{Au}}^2)(\epsilon_d + \epsilon_{\mathrm{Au}})} \times Q^{\mathrm{Co}}, \qquad (4)$$

where t_{Co} and h are the thickness and depth of the Co layer, respectively; k_z^{Au} is the z component of the SPP wave vector inside the metal; ϵ_{Au} and ϵ_d are the dielectric constants of Au and of the dielectric medium on top of the metallic trilayer; k_0 is the wave vector of light in vacuum; k_{sp}^0 corresponds to the SPP wave vector of a semi-infinite metal-dielectric interface;[35] and Q^{Co} is the Co magneto-optical parameter. To get an insight on the main parameters governing Δk_{sp} behavior, we can also employ the following approximation valid in the long-wavelength regime ($\epsilon_d \ll \epsilon_{\mathrm{Au}}$):

$$\begin{aligned}\Delta k_{sp} &\approx -2t_{\mathrm{Co}} e^{-2hk_z^{\mathrm{Au}}} \times \frac{k_0^2 \epsilon_d^2}{\epsilon_{\mathrm{Au}}} \times Q^{\mathrm{Co}} \\ &\equiv A^{\mathrm{str}} \times B^{\mathrm{plasm}} \times Q^{\mathrm{Co}}. \qquad (5)\end{aligned}$$

We can split both Eqs. (4) and (5) into three terms: a structural term A^{str}, a purely optical or plasmonic term B^{plasm}, and a MO term Q^{Co}. The structural term A^{str} is governed by geometric parameters regarding the structure (t_{Co} and h) and the z component of the SPP wave vector inside the metal, k_z^{Au}, which is also associated with the exponential decay of the SPP electromagnetic field intensity inside the metal layer mentioned before hardly depends on the wavelength, so it will not be further taken into account. The plasmonic term B^{plasm} includes all the optical parameters of the system except for those related to the ferromagnetic layer: ϵ_{Au}, ϵ_d (1 in the case analyzed here), and k_0. Thus, this term takes into account the properties of the surface plasmon polariton supported by the system for each wavelength. Finally, the MO properties of our ferromagnetic layer appear in the last term through the magneto-optical parameter Q, defined as $Q^{\mathrm{Co}} = i\epsilon_{yz}^{\mathrm{Co}}/\epsilon_{xx}^{\mathrm{Co}}$ (for $\epsilon_{xx}^{\mathrm{Co}}$ and $\epsilon_{yz}^{\mathrm{Co}}$ the optical and magneto-optical constants of Co, respectively). The spectral behavior of Δk_{sp} is therefore determined by Q^{Co} and B^{plasm}, whose dependencies on the wavelength are plotted in Figs. 3(a) and 3(b), respectively. Figure 3(b) shows the plasmonic term in the exact expression of Eq. (4) as well as the long-wavelength approximation [Eq. (5)]. As can be seen, the approximation is very good beyond 700 nm.

From the results plotted in Figs. 3(a) and 3(b) we can establish that the spectral behavior of Δk_{sp} in our AuCoAu magnetoplasmonic multilayers is dominated by the plasmonic term: The absolute value of Q increases with the wavelength while the plasmonic term shows the same decreasing behavior as Δk_{sp} as well as the presence of a small peak in the real part for small wavelengths. This shows that the evolution of the SPP properties with the wavelength is very important to determine the possible magnetic modulation achieved.

A significant SPP property is the SPP field vertical spreading, which affects the amount of field reaching the ferromagnetic layer. Actually, it has already been demonstrated that when covering the metallic multilayers with dielectric films of different thickness, the magnetic field induced modulation of the SPP wave vector evolves in the same way as the redistribution of the SPP electromagnetic field.[16] The same mechanism, as a function of the wavelength, can be invoked here. In fact, we can rewrite Eq. (4) so that the amount of SPP field inside the Co layer appears explicitly. For that, we refer to the SPP magnetic field component intensity $|H_y|^2$ at the Co layer position. This magnitude is normalized so that for each wavelength the integral of $|H_y|^2$ along the z axis is equal to 1 (the energy density is the same in all cases). Taking into account that for a Au/dielectric semi-infinite interface the normalized SPP magnetic field can be written as $[2k_z^{\mathrm{Au}} k_z^d/(k_z^{\mathrm{Au}} + k_z^d)]^{1/2} e^{-k_z^{\mathrm{Au}} z}$, with k_z^{Au} and k_z^d the z components of the SPP wave vector in the metal and

dielectric, respectively, and using some arithmetic, we obtain the following expression:

$$\Delta k_{sp} \approx t_{\mathrm{Co}} \times \frac{k_0 \epsilon_d \epsilon_{\mathrm{Au}} \sqrt{-(\epsilon_d + \epsilon_{\mathrm{Au}})}}{\epsilon_d^2 - \epsilon_{\mathrm{Au}}^2} \left| H_y^{\mathrm{Co}} \right|^2 \times Q^{\mathrm{Co}}. \quad (6)$$

In Fig. 3(c), we plot $|H_y^{\mathrm{Co}}|^2$ as a function of the wavelength. The SPP field does indeed decrease with the wavelength, as Δk_{sp} does, confirming that the penetration of the SPP in the MO layer is the main parameter to take into account in the spectral behavior of Δk_{sp}. The SPP field, however, does not reproduce all the details found in the spectral evolution of Δk_{sp}^r and Δk_{sp}^i. This is due to the influence of other optical parameters, as can be seen from Eq. (6). The term containing the proportionality to the SPP field at the Co layer interface contains some other optical factors whose particular spectral response slightly modifies the pure decay of the field with the wavelength, to finally define the obtained spectral shape of Δk_{sp} (real and imaginary parts).

This information on the spectral dependence of SPP electromagnetic field confinement, implicit in B^{plasm}, is also contained in the dispersion relation. If we consider the separation of the SPP wave vector from the light line, $k_{sp}^0 - k_0$, the bigger separation occurring at shorter wavelengths implies a stronger evanescent decay and therefore a higher confinement. As a consequence, the magnitude $k_{sp}^0 - k_0$ is also able to describe the spectral shape of Δk_{sp}, and we have found that it does it in a very accurate way for both Δk_{sp}^r and Δk_{sp}^i for our AuCoAu trilayered system, as shown in Fig. 3(d). Summarizing, for longer wavelengths the SPP wave vector is closer to the light line and thus the associated electromagnetic field is more spread out of the interface, while for smaller wavelengths k_{sp} increases and the SPP field becomes more confined to the interface and the presence of the Co layer is strongly felt. Our results show that this effect has a bigger influence on Δk_{sp} than the increase of Q^{Co} with wavelength.

V. EXTENSION TO OTHER FERROMAGNETIC METALS

The discussion performed above regarding the spectral evolution of the magnetic field driven modulation of SPP wave vector for the particular AuCoAu trilayer system could be, in principle, extended to the other ferromagnetic metals, Fe and Ni, as the different parameters, k_{sp} properties and Q, evolve in a similar way. The right axis of Fig. 4(b) shows the calculated values of Δk_{sp}^r and Δk_{sp}^i for trilayers of Au/FerromagneticMetal/Au with a ferromagnetic metal layer of 6 nm and $h = 15$ nm. To make the analysis as general as possible, instead of employing optical and MO dielectric constants experimentally determined in our laboratory, we have chosen in this case to use well-established values that can be found in the literature for the bulk forms of the analyzed materials: Au, dielectric constant;[36] Fe and Co, optical[37] and MO[38] constants; and Ni, optical[39] and MO[40] constants. In Fig. 4(a), the corresponding magneto-optical parameters Q for Fe, Co, and Ni are shown. As can be seen in Fig. 4(b), the greatest absolute values of modulation are obtained for Fe, and Ni provides the lowest values, in agreement with the values of Q parameter for each metal. Regarding the evolution with wavelength, Δk_{sp} behaves in the expected decreasing way,

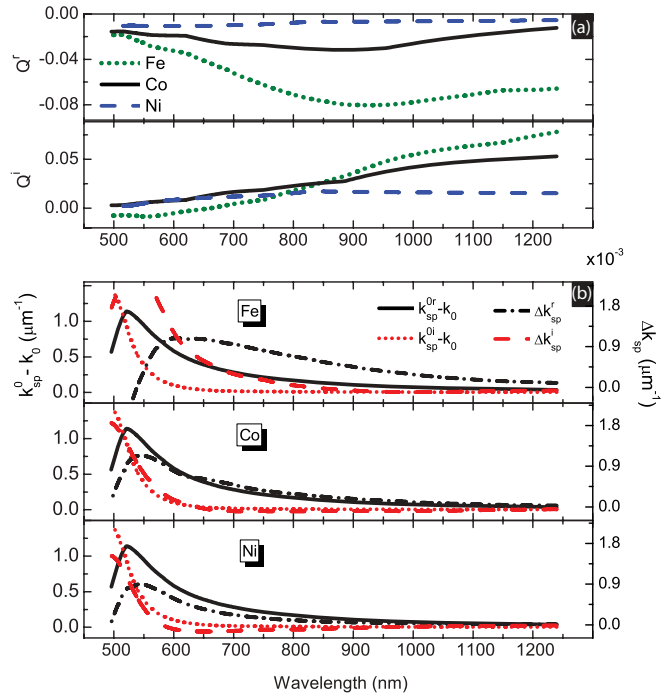

FIG. 4. (Color online) (a) Wavelength dependence of the magneto-optical parameter Q for the three ferromagnetic metals Fe (dotted green line), Co (solid black line), and Ni (blue dashed line), calculated from typical optical and magneto-optical constants for the bulk materials referred to in the literature: $\epsilon_{xx}^{\mathrm{Fe}}$ (Ref. 37), $\epsilon_{yz}^{\mathrm{Fe}}$ (Ref. 38), $\epsilon_{xx}^{\mathrm{Co}}$ (Ref. 37), $\epsilon_{yz}^{\mathrm{Co}}$ (Ref. 38), $\epsilon_{xx}^{\mathrm{Ni}}$ (Ref. 39), and $\epsilon_{yz}^{\mathrm{Ni}}$ (Ref. 40). (b) Right axis: Dependence on wavelength of the real part (black dash-dot line) and the imaginary part (red dashed line) of calculated Δk_{sp} for trilayers of Au/FerromagneticMetal/Au with $h = 15$ nm and $t_{\mathrm{Ferro}} = 6$ nm, where Fe (top panel), Co (middle panel), and Ni (bottom panel) are the ferromagnetic metal. Left axis: Comparison of the calculated Δk_{sp} with the separation of the SPP wave vector from the light line (real part in black solid line and imaginary part in red dotted line). The Q parameter used in the calculations is the one shown in part (a) of the figure.

even for increasing values of Q, confirming the predominance of the plasmonic term to determine this evolution. Figure 4(b) also compares the evolution of Δk_{sp} with the distance of k_{sp}^0 to the light line (left axis), with again a good agreement between both quantities. The matching between Δk_{sp} and $k_{sp}^0 - k_0$ trends is slightly worse in the case of Fe, mainly at small wavelengths, because of the stronger dependency of Q^{Fe} with wavelength in this regime, which gives rise to a stronger convolution of the product of the MO and the plasmonic term in Eq. (5) for this ferromagnetic metal.

It is well known that the propagation distance of surface plasmon polaritons increases with wavelength, so that longer wavelengths would provide a higher flexibility in the design of magnetic field driven plasmonic devices. For example, in the case of magnetoplasmonic modulators based on interferometers, the modulated intensity I_{mp} is proportional to the product of Δk_{sp} times the slit-groove distance d,[15,16] so that higher modulations can be obtained by increasing this distance. Therefore, in order to evaluate the optimal spectral range for the performance of magnetoplasmonic modulators, the

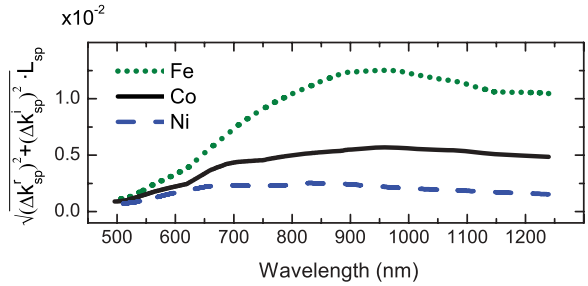

FIG. 5. (Color online) Spectral evolution of the figure of merit $\sqrt{(\Delta k_{sp}^r)^2 + (\Delta k_{sp}^i)^2} \times L_{sp}$ for the same Au/FerromagneticMetal/Au trilayers as in Fig. 4, with the ferromagnetic metal being Fe (dotted green line), Co (solid black line), and Ni (blue dashed line).

product $\sqrt{(\Delta k_{sp}^r)^2 + (\Delta k_{sp}^i)^2} \times L_{sp}$, with L_{sp} being the length at which the surface plasmon polariton intensity decays a factor $1/e$, constitutes an adequate figure of merit.[16] Figure 5 shows this figure of merit for the three Au/FerromagneticMetal/Au trilayers with Fe, Co, and Ni. The best performance in absolute terms is again obtained by Fe, Ni being the worst one, in agreement with the amount of MO response strength as indicated by Q. In the wavelength region with $\Delta k_{sp}^i > \Delta k_{sp}^r$, $\lambda_0 < 520$ nm, the figure of merit is too small since the propagation distance of the SPP is almost zero. In the spectral range where SPPs start having propagation distances of a few microns and therefore could be employed in photonic devices (SPP propagation distance $L_{sp} > 3$ μm at $\lambda_0 > 600$ nm for a Au/Co/Au trilayer with the Co layer placed at $h = 15$ nm), the figure of merit increases and achieves its maximum value at around 1 μm. At these wavelengths, as was seen from Fig. 2, both real and imaginary components of the modulation are relevant. Finally, for wavelengths $\lambda_0 > 1$ μm, the figure of merit decreases a little, seeming to reach a saturation value.

Taking the values of Fig. 5 into consideration, a magneto-plasmonic modulator consisting of a Au/Fe/Au interferometer with a separation distance of $3L_{sp}$ (achievable from our experimental experience) and covered with a dielectric with $\varepsilon_d = 2$ (see Ref. 16) could provide intensity modulations ($\Delta I/I = 2|\Delta k|L_{sp}$)[15] of around 12% in the optimal spectral range (950 nm). This value is not far from other integrated plasmonic modulator performances reported in the literature based on thermo-optical or electro-optical effects.[14,18] These examples have the advantage of being already implemented in SPP waveguide configurations, while the interferometer geometry is still an extended one. However, magneto-optical effects offer the advantage of higher switching speed.

VI. CONCLUSIONS

We have determined both the real and the imaginary parts of the magnetic field induced modification of the SPP wavevector for Au/FerromagneticMetal/Au magnetoplasmonic systems. It has been shown that the real part is the dominating component in most of the spectral range, although at longer wavelengths the values of both components approach and the imaginary part has to be taken into account to appropriately describe the system response. The spectral dependence of the SPP wave vector modulation has been characterized, and it shows a decreasing behavior with wavelength. By means of an analytical expression for Δk_{sp} obtained in the approximation of a very thin ferromagnetic metal layer, we have established that this spectral trend is due to the evolution of the SPP properties with wavelength. These properties come from the vertical confinement of the SPP field, which can be qualitatively described by the evolution of the separation between the SPP wave vector and the light line. The spectral behavior has been also calculated for Fe and Ni, evolving the same way as for Co. A figure of merit combining both magnetic modulation and propagation of the SPP is also analyzed. In terms of spectral dependence, the decrease of SPP wave vector modulation is overcompensated by the increase in L_{sp} for a significant wavelength range, so that the 700 nm to 1 μm interval becomes the optimal one.

ACKNOWLEDGMENTS

We acknowledge funding from the EU (NMP3-SL-2008-214107-Nanomagma), the Spanish MICINN ("MAPS" MAT2011-29194-C02-01, "MAGPLAS" MAT2008-06765-C02-01/NAN, and "FUNCOAT" CONSOLIDER INGENIO 2010 CSD2008-00023), the Comunidad de Madrid ("MICROSERES-CM" S2009/TIC-1476), and Deutsche Forschungsgemeinschaft and Region Pays de La Loire.

APPENDIX: DERIVATION OF THE MAGNETOPLASMONIC INTERFEROGRAM EQUATION

When we apply a magnetic field, a variation of the transmitted intensity at each point of the slit associated with the modulation of the SPP wave vector takes place: $\Delta I = I(+M) - I(-M) \equiv I_{mp}$. In a first-order approximation (valid for $\Delta k_{sp} d \ll 1$), this ΔI is the derivative of the transmitted intensity $I = A_r^2 + A_{sp}^{g\,2} e^{-2k_{sp}^i d} + 2A_r A_{sp}^g e^{-k_{sp}^i d} \cos(k_{sp}^r d + \varphi_0)$ with respect to the magnetic field:

$$\begin{aligned} I_{mp} = &-4A_{sp}^{g\,2} e^{-2k_{sp}^{0i} d} \Delta k_{sp}^i d \\ &- 4A_r A_{sp}^g e^{-k_{sp}^{0i} d} \big[\Delta k_{sp}^i d \cos\left(k_{sp}^{0r} d + \varphi_0\right) \\ &+ \Delta k_{sp}^r d \sin\left(k_{sp}^{0r} d + \varphi_0\right)\big]. \end{aligned} \tag{A1}$$

As can be seen, this expression consists of a first small offset term, a component in phase with the optical interferogram associated with Δk_{sp}^i, and a $\pi/2$-shifted component due to Δk_{sp}^r. Neglecting the offset term, and applying some trigonometry, Eq. (A1) can be expressed as

$$\begin{aligned} I_{mp} = &-4A_r A_{sp}^g e^{-k_{sp}^{0i} d} d \sqrt{\left(\Delta k_{sp}^r\right)^2 + \left(\Delta k_{sp}^i\right)^2} \\ &\times \sin\left(k_{sp}^{0r} d + \varphi_0 + \phi\right), \end{aligned} \tag{A2}$$

where ϕ is defined as $\tan\phi = \Delta k_{sp}^i / \Delta k_{sp}^r$. This ϕ phase can be determined as the shift between the maxima (or minima) of the optical interferogram and the zeros of the magnetoplasmonic one [see zoom in Fig. 1(b) of the main text].

The I_{mp} signal can be normalized by the amplitude contrast of the optical intensity I, $I_{\text{contrast}} = 4A_r A_{sp}$, resulting in

$$I_{mp}^{\text{norm}} = -d\sqrt{\left(\Delta k_{sp}^r\right)^2 + \left(\Delta k_{sp}^i\right)^2}\sin\left(k_{sp}^{0r}d + \varphi_0 + \phi\right). \quad \text{(A3)}$$

The amplitude of this normalized I_{mp} is then proportional to $\sqrt{(\Delta k_{sp}^r)^2 + (\Delta k_{sp}^i)^2} \times d$. By determining the amplitude of I_{mp}^{norm} and ϕ, we can obtain Δk_{sp}^r and Δk_{sp}^i.

*diana.martin@imm.cnm.csic.es; also at International Iberian Nanotechnology Laboratory, 4710-229 Braga, Portugal.
†Now at Institut des Molécules et Matériaux du Mans, UMR CNRS 6283, Université du Maine, 72085 Le Mans cedex, France.
‡Now at Joint Quantum Institute, National Institute of Standards and Technology and University of Maryland, Gaithersburg, MD, USA.
§Now at Institute of Physics, Chemnitz University of Technology, D-09107 Chemnitz, Germany.
‖maria-ujue.gonzalez@csic.es

[1]W. L. Barnes, A. Dereux, and T. W. Ebbesen, Nature **424**, 824 (2003).
[2]E. Ozbay, Science **311**, 189 (2006).
[3]T. W. Ebbesen, C. Genet, and S. I. Bozhevolnyi, Phys. Today **61**(5), 44 (2008).
[4]D. K. Gramotnev and S. I. Bozhevolnyi, Nat. Photonics **4**, 83 (2010).
[5]B. Berini and I. De Leon, Nat. Photonics **6**, 16 (2012).
[6]A. V. Krasavin, K. F. MacDonald, N. I. Zheludev, and A. V. Zayats, Appl. Phys. Lett. **85**, 3369 (2004).
[7]T. Nikolajsen, K. Leosson, and S. I. Bozhevolnyi, Appl. Phys. Lett. **85**, 5833 (2004).
[8]D. Pacifici, H. J. Lezec, and H. A. Atwater, Nat. Photonics **1**, 402 (2007).
[9]R. A. Pala, K. T. Shimizu, N. A. Melosh, and M. L. Brongersma, Nano Lett. **8**, 1506 (2008).
[10]M. J. Dicken, L. A. Sweatlock, D. Pacifici, H. J. Lezec, K. Bhattacharya, and H. A. Atwater, Nano Lett. **8**, 4048 (2008).
[11]J. A. Dionne, K. Diest, L. A. Sweatlock, and H. A. Atwater, Nano Lett. **9**, 897 (2009).
[12]K. F. MacDonald, Z. L. Sámson, M. I. Stockman, and N. I. Zheludev, Nat. Photonics **3**, 55 (2009).
[13]V. V. Temnov, K. Nelson, G. Armelles, A. Cebollada, T. Thomay, A. Leitenstorfer, and R. Bratschitsch, Opt. Express **17**, 8423 (2009).
[14]J. Gosciniak, S. I. Bozhevolnyi, T. B. Andersen, V. S. Volkov, J. Kjelstrup-Hansen, L. Markey, and A. Dereux, Opt. Express **18**, 1207 (2010).
[15]V. V. Temnov, G. Armelles, U. Woggon, D. Guzatov, A. Cebollada, A. García-Martín, J. García-Martín, T. Thomay, A. Leitenstorfer, and R. Bratschitsch, Nat. Photonics **4**, 107 (2010).
[16]D. Martín-Becerra, J. B. González-Díaz, V. V. Temnov, A. Cebollada, G. Armelles, T. Thomay, A. Leitenstorfer, R. Bratschitsch, A. García-Martín, and M. U. González, Appl. Phys. Lett. **97**, 183114 (2010).
[17]A. Agrawal, C. Susut, G. Stafford, U. Bertocci, B. McMorran, H. J. Lezec, and A. A. Talin, Nano Lett. **11**, 2774 (2011).
[18]S. Randhawa, S. Lachèze, J. Renger, A. Bouhelier, R. E. de Lamaestre, A. Dereux, and R. Quidant, Opt. Express **20**, 2354 (2012).
[19]J. J. Brion, R. F. Wallis, A. Hartstein, and E. Burstein, Phys. Rev. Lett. **28**, 1455 (1972).
[20]K. W. Chiu and J. J. Quinn, Phys. Rev. Lett. **29**, 600 (1972).
[21]R. F. Wallis, J. J. B. E. Burstein, and A. Hartstein, Phys. Rev. B **9**, 3424 (1974).
[22]J. B. Khurgin, Appl. Phys. Lett. **89**, 251115 (2006).
[23]W. V. Parys, B. Moeyersoon, D. V. Thourhout, R. Baets, M. Vanwolleghem, B. Dagens, J. Decobert, O. L. Gouezigou, D. Make, R. Vanheertum, and L. Lagae, Appl. Phys. Lett. **88**, 071115 (2006).
[24]B. Sepúlveda, L. Lechuga, and G. Armelles, J. Lightwave Technol. **24**, 945 (2006).
[25]Z. Yu, G. Veronis, Z. Wang, and S. Fan, Phys. Rev. Lett. **100**, 023902 (2008).
[26]J. Montoya, K. Parameswaran, J. Hensley, M. Allen, and R. Ram, J. Appl. Phys. **106**, 023108 (2009).
[27]A. V. Kimel, A. Kirilyuk, P. A. Usachev, R. V. Pisarev, A. M. Balbashov, and Th. Raising, Nature (London) **435**, 655 (2005).
[28]J. B. González-Díaz, A. García-Martín, G. Armelles, J. M. García-Martín, C. Clavero, A. Cebollada, R. A. Lukaszew, J. R. Skuza, D. P. Kumah, and R. Clarke, Phys. Rev. B **76**, 153402 (2007).
[29]E. Ferreiro-Vila, J. B. González-Díaz, R. Fermento, M. U. González, A. García-Martín, J. M. García-Martín, A. Cebollada, G. Armelles, D. Meneses-Rodríguez, and E. M. Sandoval, Phys. Rev. B **80**, 125132 (2009).
[30]C. Clavero, K. Yang, J. R. Skuza, and R. A. Lukaszew, Opt. Express **18**, 7743 (2010).
[31]E. Ferreiro-Vila, M. Iglesias, E. Paz, F. J. Palomares, F. Cebollada, J. M. González, G. Armelles, J. M. García-Martín, and A. Cebollada, Phys. Rev. B **83**, 205120 (2011).
[32]J. Renger, S. Grafström, and L. M. Eng, Phys. Rev. B **76**, 045431 (2007).
[33]J. B. González-Díaz, Ph.D. thesis, Universidad Autónoma de Madrid, Spain, 2010.
[34]Although this peak has not been experimentally confirmed since the very short plasmon propagation distance at wavelengths below 530 nm has prevented the measurement, the good accord between measurements and simulations in the rest of the spectral range allows us to trust the presence of this peak.
[35]S. A. Maier, *Plasmonics: Fundamentals and Applications* (Springer, Berlin, 2007).
[36]P. B. Johnson and R. W. Christy, Phys. Rev. B **6**, 4370 (1972).
[37]P. B. Johnson and R. W. Christy, Phys. Rev. B **9**, 5056 (1974).
[38]G. S. Krinchik, J. Appl. Phys. **35**, 1089 (1964).
[39]E. D. Palik, *Handbook of Optical Constants of Solids* (Academic Press, San Diego, 1998).
[40]K. Mok, G. J. Kovács, J. McCord, L. Li, M. Helm, and H. Schmidt, Phys. Rev. B **84**, 094413 (2011).